Halogen heterogeneity in the subcontinental lithospheric mantle revealed by I/Br ratios in kimberlites and their mantle xenoliths from South Africa, Greenland, China, Siberia, Canada, and Brazil

Chiaki Toyama[1,2], Hirochika Sumino[3,*], Nobuaki Okabe[2,4], Akira Ishikawa[5], Junji Yamamoto[6], Ichiro Kaneoka[7] and Yasuyuki Muramatsu[2]

1 Institute of Geology and Geoinformation, Geological Survey of Japan, The National Institute of Advanced Industrial Science and Technology (AIST), Ibaraki, 237-0061, Japan
2 Department of Chemistry, Gakushuin University, Tokyo, 171-8588, Japan
3 Department of General Systems Studies, Graduate School of Arts and Sciences, The University of Tokyo, Tokyo, 153-8902, Japan
4 Institute for Environmental Sciences, Aomori, 039-3212, Japan
5 Department of Earth and Planetary Sciences, School of Science, Tokyo Institute of Technology, Tokyo 152-8851, Japan
6 The Hokkaido University Museum, Hokkaido, 060-0810, Japan
7 Earthquake Research Institute, The University of Tokyo, Tokyo, 113-0032, Japan

*Correspondence

Chiaki Toyama: c-toyama@aist.go.jp
Hirochika Sumino: sumino@igcl.c.u-tokyo.ac.jp
Nobuaki Okabe: okabe.nobuaki@jaea.go.jp
Akira Ishikawa: akr@eps.sci.titech.ac.jp
Junji Yamamoto: jyama@museum.hokudai.ac.jp
Ichiro Kaneoka: Ikaneoka@aol.com
Yasuyuki Muramatsu: deceased

Abstract

In order to investigate the halogen heterogeneity in the subcontinental lithospheric mantle (SCLM), we measured the concentrations of Cl, Br, and I in kimberlites and their mantle xenoliths from South Africa, Greenland, China, Siberia, Canada, and Brazil. The samples can be classified into two groups based on halogen

ratios: a high-I/Br group (South Africa, Greenland, Brazil, and Canada) and a low-I/Br group (China and Siberia). The halogen compositions were examined with the indices of crustal contamination using Sr and Nd isotopes and incompatible trace elements. The results indicate that the difference between the two groups was not due to different degrees of crustal contamination, but from the contributions of different mantle sources. The low-I/Br group has a similar halogen composition to seawater-influenced materials such as fluids in altered oceanic basalts and eclogites, and fluids associated with halite precipitation from seawater. We conclude that the halogens of the high-I/Br group are most likely derived from a SCLM source metasomatized by a fluid derived from subducted serpentinite, whereas those of the low-I/Br group are derived from a SCLM source metasomatized by a fluid derived from seawater-altered oceanic crust. The SCLM beneath Siberia and China could be an important reservoir of subducted, seawater-derived halogens, while such role of SCLM beneath South Africa, Greenland, Canada and Brazil seems limited.

Keywords: halogens, kimberlite, subcontinental lithospheric mantle, subduction, metasomatism

1. Introduction

Subduction of oceanic plates carries large amounts of surface materials into the Earth's interior. Among these subducted materials, water released from the subducting oceanic plate plays an important role in the dynamic processes occurring in the mantle wedge, including: (1) the generation of arc magmas beneath subduction zones owing to the lowering of the melting temperature of the wedge mantle peridotite (e.g., Ulmer, 2001); (2) generation of deep earthquakes by weakening of the mechanical strength of the subducted lithosphere and coupling between the subducted slab and the superjacent mantle wedge (e.g., Seno, 2009); and (3) control of mantle rheology that affects the efficiency of mantle convection (e.g., Bolfan-Casanova, 2005).

Most of the water carried by plate subduction is bound in hydrous minerals in altered and metamorphosed igneous oceanic crusts and sediments (e.g., Bebout, 1996). Almost all of the pore water (water trapped in pore spaces in sediments and oceanic crust) is expelled from the plate subducted to a depth of 5 km and returned to the surface, resulting in deep seepage within accretionary prisms (e.g., Jarrard, 2003). However, deep subduction of the marine pore fluid has been suggested based on the

noble gas isotopic data from continental well gases (Holland and Ballentine, 2006) and halogen compositions obtained from exhumed mantle wedge peridotites and metasomatized mantle xenoliths (Sumino et al., 2010; Broadley et al., 2016; Kobayashi et al., 2017). The serpentinized lithospheric mantle in a subducted oceanic plate has been suggested as the transport medium of the marine pore-fluid-derived noble gases and halogens (Sumino et al., 2010; Kendrick et al., 2011, 2013, 2017; Kobayashi et al., 2017). However, little is known about the behavior of halogens during the subduction processes and their fate in the Earth's mantle.

Halogens (chlorine (Cl), bromine (Br), and iodine (I)) have high partition coefficients in aqueous fluids (Bureau et al., 2000). Pore fluids are enriched in halogens as they are originated from seawater; however, the high content of I (and of Br to a lesser extent) in organic matter in sediments results in higher I/Cl and Br/Cl ratios in the pore fluids than seawater (Riley and Skirrow, 1975; Déruelle et al., 1992; Jambon et al., 1995; Muramatsu and Wedepohl, 1998; Bureau et al., 2000; Johnson et al., 2000). The halogen elemental ratios are distinctive in the seawater, pore water, sediment, altered oceanic crust, and peridotite. The halogens are, therefore a useful tool for tracing the water cycle in subduction zones (e.g., Sumino et al., 2010; Broadley et al., 2016; Kobayashi et al., 2017).

Kimberlites are igneous rocks, majority of which occur within the Archean cratons and surrounding mobile belts, and are produced via explosive eruptions mainly in the Precambrian age (e.g., Sparks, 2013). Because of the presence of diamonds in some kimberlites, kimberlite magmas have been regarded as being derived from a source in the mantle deeper than 150 km (e.g., Ringwood et al., 1992). Compared to the other ultramafic rocks, kimberlites are extremely rich in volatiles which results in a rapid ascent, enabling diamonds to be transported to the surface before their graphitization (e.g., Sparks, 2013).

Kimberlites have been conventionally classified into Group I and Group II based on Sr-Nd-Pb isotope systematics (Smith, 1983). In the isotopic classification by Smith (1983), Group I kimberlites are slightly less radiogenic in terms of their Sr isotope, and more radiogenic in terms of their Nd isotope compositions than the present-day bulk Earth. In this regard, they show similarity to ocean island basalts (OIB). Smith (1983) demonstrated the possible genetic link of the Group I kimberlites and a deep mantle source. Based on comparison of eruption ages and locations of the kimberlites with plate reconstructions, it has been suggested that mantle plumes tapping the core-mantle boundary beneath Africa and south Pacific may be responsible for kimberlite genesis (Torsvik et al., 2010). Woodhead et al. (2019) compiled Nd and Hf

isotope data of the Group I kimberlites with careful filtering based on major and trace element compositions and revealed that the mantle reservoir from which those kimberlites originate from is a single homogeneous deep-seated reservoir with a pristine isotope signature, which has been isolated from mantle convection over at least 2.5 billion years. In addition, studies of the noble gas isotopes in Group I kimberlites showed that kimberlite magmas have similar noble gas compositions as the ocean island basalts derived from deep mantle plumes (Sumino et al., 2006; Tachibana et al. 2006).

In contrast, Group II kimberlites, which were also termed "orangeites" after their occurrence (Mitchell 2012), have highly radiogenic Sr isotope compositions relative to the bulk Earth and have been associated with a direct derivation from the subcontinental lithospheric mantle (SCLM) (e.g., Smith, 1983). In recent years, the Group II kimberlites are petrogenetically classified as olivine lamproites and excluded from "archetypal" kimberlites (e.g., Pearson et al., 2019). Although the origin of the Group II kimberlites is not well constrained, it would be an enriched SCLM source metasomatized by melts or fluids associated with ancient subduction (Becker and le Roex, 2005) or by volatile-rich components derived from mantle upwelling related to a plume or back-arc extension (Mirnejad et al., 2006).

The initiation of melting to form Group I kimberlites is considered to take place below SCLM. Although the incipient melt entering the base of SCLM would have been carbonatitic, during the ascent in SCLM the melt consumes silicate minerals (orthopyroxene) in surrounding mantle peridotite to evolve to silica-rich composition as observed as kimberlite magma at the surface (Kamenetsly et al., 2008; Russel et al., 2012). Since the source mantle of MORB and OIB is indistinguishable in terms of Br/Cl and I/Cl ratios (Kendrick et al., 2017), the MORB- and OIB-like halogen ratios of kimberlite magma would have been modified by the interaction with SCLM. In this regard, the study of halogens in kimberlites can provide important information related to the deep halogen composition of SCLM. In order to investigate the characteristics of halogens in SCLM, we have examined the relative compositions of Cl, Br, and I of kimberlite samples and their mantle xenoliths collected from South Africa, Greenland, China, Siberia, Canada, and Brazil.

2. Samples

We analyzed the concentrations of Cl, Br, and I in 27 kimberlite samples (bulk rock) from six localities (South Africa, Greenland, China, Siberia, Canada, and Brazil) and four mantle xenoliths of the kimberlites from South Africa and Siberia, as described below. Photos of thin sections of the samples are provided as Supplementary materials.

The South African kimberlites and their xenolith (peridotite) samples were collected from seven locations surrounding the Kimberley area (Newland, Benfontein, Frank-Smith, De Beers, Klipfontein and Wesselton). The Kimberley cluster of kimberlite pipes constitutes the type locality for kimberlite. The detailed geology of the individual pipes has been described comprehensively by Clement (1982). Numerous studies have been conducted on the Kimberley kimberlites (e.g., Clement, 1982; Smith, 1983; Muramatsu and Wedepohl, 1985; Chalapathi Rao et al., 2004). The Rb–Sr, U–Pb and Pb–Pb model ages of 80–114 Ma for kimberlites from the Kimberley area were reported (e.g., Kramers and Smith, 1983). The South African kimberlite samples used in this study were also used for our previous studies (Muramatsu, 1983; Toyama et al., 2012) and classified into Group I and II by Toyama et al. (2012) based on Nd-Sr isotopic compositions. The sample IDs of the samples used in this study are the same as those used in Muramatsu (1983) and Toyama et al. (2012). In addition, F and Cl were analyzed in a selection of samples by Muramatsu (1983). The details of the geology of the areas where the samples were collected have been previously described by Muramatsu and Wedepohl (1985). The kimberlite samples studied contain olivine (serpentine), pyroxenes, phlogopite, calcite, dolomite (only in K-2), and garnet (only in K-1 and K-8) as major minerals, and magnetite, ilmenite, spinel, pyrite, Fe-Ni and Cu-S ores, perovskite, rutile, barite and plagioclase as accessory minerals (Muramatsu, 1983). The samples are variably altered exhibiting partial to near-complete replacement of the olivine by serpentine and/or clay minerals, but a subset of samples are very fresh.

The Greenland kimberlite samples were collected from the Sarfartoq region of the North Atlantic Craton. The details of the geology of these provinces have been described by Gaffney et al. (2007). Kimberlites in this area erupted at ca. 600 Ma (e.g., Gaffney et al., 2007). The Hf-Nd isotopic compositions and the concentrations of the major and the trace elements in the West Greenland kimberlite samples used in this study are reported by Gaffney et al. (2007). These samples are classified as Group I kimberlites. The sample numbers of the west Greenland samples used in this study are the same as those used in Gaffney et al. (2007). The samples contain olivine, phlogopite, and ilmenite as major minerals, and minor clinopyroxene and calcite. The olivine is very abundant (up to 70%), thus some of them are likely of accumulated or xenocrystic origin (Gaffney et al., 2007).

The Siberian kimberlites and their xenolith samples (peridotite) were collected from the Udachnaya-East kimberlite pipe in Yakutia of the Siberian Craton. The studied kimberlite samples are exceptionally fresh so that there is almost no secondary serpentinization of olivine crystals and even native halite crystals were found (Mass et

al., 2005; Kamenetsky et al., 2004, 2012). The emplacement age of the pipe has been reported as ca. 347 Ma (Mass et al., 2005). The Sr and Nd isotopic compositions of samples from the pipe are typical of Group I kimberlites (e.g., Kamenetsky et al., 2004; Mass et al., 2005). In addition, studies on the noble gas isotopes in the olivine phenocrysts in the Udachnaya-East kimberlites showed that the kimberlite magma has noble gas characteristics similar to those of ocean island basalts (Sumino et al., 2006). The sample numbers of the Siberian samples used in this study are the same as those used in previous studies (Kamenetsky et al., 2012; Mass et al., 2005). The samples contain abundant olivine grains (up to 40–50 vol.%) in the groundmass composed of phlogopite, monticellite, plagioclase, sodalite, perovskite, spinel, titanomagnetite, pyrrhotite, djerfisherite, Na-K chlorides, Na-Ca sulfates, apatite, and calcite (Kamenetsky et al., 2012; Mass et al., 2005).

The Chinese kimberlite samples were collected from Liaoning (Wafangdian area) and Shandong (Jining and Mengyin areas) of the North China Craton. The details of the geology of these provinces have been described by Li et al. (2011). The Shandong (Mengyin area) kimberlite province has many petrological and mineralogical features in common with the 475 Ma kimberlites at Fuxian in Lianong province, located 550 km southwest of the Mengyin area (Dobbs et al., 1994). The emplacement age of the Paleozoic kimberlites in the North China Craton of approximately 480 Ma is supported by other studies on Chinese kimberlites (e.g., Yang et al., 2009; Li et al., 2011). The Chinese kimberlite samples used in this study were also used for our previous study (Toyama et al., 2012), which reported the Sr-Nd isotopic compositions and the concentrations of the major and trace elements. Toyama et al. (2012) classified the Liaoning kimberlites and the Shandong kimberlites as Transitional and Group I, respectively, based on the Sr and the Nd isotopic compositions. This is consistent with the results of Dobbs et al. (1994) and Lu et al. (1995). The sample IDs of the Chinese samples are the same as those in our previous study (Toyama et al., 2012). Olivines in the three samples from Shandong were serpentinized, while serpentinized olivines in the two samples from Liaoning were further altered and partly replaced by fine-grained clay minerals (Toyama et al., 2012).

The Canadian kimberlite samples were collected from Somerset Island at the northern margin of the Canadian craton. The other geochemical data for the particular samples have not yet been published. The kimberlites in this area have been described by Mitchell (1976). Wu et al. (2010) reported a U–Pb model age of 90–105 Ma for the kimberlites. A petrological study indicated that most of the Somerset Island kimberlites belong to hypabyssal root zone (Mitchell and Meyer 1980). The studied samples consist

of abundant olivine macrocrysts (~50 vol.%) and fined-grained magmaclasts (~40 vol.%) in dolomite matrix (~10% vol.).

The Brazilian kimberlite samples were collected from borehole cores from Minas Gerais. The other geochemical data for these samples also have not yet been published. The majority of the radiometric ages of the other kimberlites in Minas Gerais were reported as 80–120 Ma (e.g., Meyer et al., 1994). The kimberlite samples studied here display different extents of alteration: less-altered sample (X218) contains abundant fresh olivine, while olivine in the other (X219) exhibits near-complete replacement by serpentine and/or clay minerals.

3. Analytical Method

The analytical method used in this study consists of the following steps: (1) the separation of halogen from the sample into an aqueous solution by pyrohydrolysis, and (2) the measurement of the halogen elements in the solution by ion chromatography (IC) and inductively coupled plasma mass spectrometry (ICP-MS).

In step one, pyrohydrolysis used in this study is an improved method of that reported by Muramatsu and Wedepohl (1998), which was developed to separate I from silicates. We have optimized the heating temperature, heating time, trap solution etc. to extract Cl, Br, and I. About 500 mg of powdered sample was mixed with 500 mg of V_2O_5 (99%, Kanto Chemical Co. Ltd.) in an alumina combustion boat (99.9% purity). Then the combustion boat containing the sample was heated at 1100 ºC or higher in a quartz tube under constant wet oxygen flow containing water vapor for 45 min. Using this procedure, halogens were volatilized and trapped by 10 mL of de-ionized water (Milli-Q, 18 MΩ). As native halite crystals have been found in Siberian kimberlite from the Udachnaya-east pipe (Mass et al., 2005; Kamenetsky et al., 2004, 2012) and halite would concentrate halogens, we leached powdered Udachnaya kimberlite samples with de-ionized water before pyrohydrolysis to test the effect of halite dissolution.

In step 2, the Cl concentrations in the trap solution were determined with IC (DIONEX ICS-1500). For Br and I, 25% ultra-pure tetra-methyl ammonium hydroxide (TMAH: Tama Chemicals) was added to the trapped solution, because Br and I dissolved in alkaline solution. The sample solutions were measured for ^{79}Br and ^{127}I by ICP-MS (Agilent 7500, 7700). To avoid the memory effect of I on the instrument, sufficient washout time was given after the measurement of a sample with a high I concentration for the signal at *m/z* 127 to return to the background level.

We validated our method by analyzing a standard reference material JB-2 (basalt) provided by the Geological Survey of Japan (GSJ). The results for all elements

agreed with the recommended or preferable values (Cl = 281 ppm, and I =49 ppb) reported by GSJ within 10% uncertainty (1σ; n = 5). The recommended or preferable value of Br is not reported by GSJ. We estimated the reference value of Br (0.7 ppm) based on the data reported by Shinonaga et al. (1994) and Korotev (1996).

4. Results

The halogen data obtained for 27 kimberlites and four of their mantle xenoliths are summarized in Table 1. Note that only one analysis was performed for the South African samples. The reason is that the halogen data in this study showed good agreement (within ± 20%) with the analyzed values using X-ray fluorescence spectrometry and the pyrohydrolysis method before the improvement (Muramatsu, 1983; Muramatsu, unpublished data). Analytical uncertainties for the other samples were defined by the standard deviation derived from results of repeated analyses (n = 2–5).

In Fig. 1, the halogen concentrations in the kimberlite and the xenolith samples are shown together with those in mid-ocean ridge basalts (MORB) and oceanic island basalts (OIB) reported by Kendrick et al. (2017). Note that only MORB and OIB data free of seawater assimilation are plotted in the figure. The bulk halogen concentrations for peridotite xenoliths in the Udachnaya kimberlites reported by Broadley et al. (2018a) are also shown for comparison. Halogen data for peridotite xenoliths in the Obnazhennaya kimberlite, which erupted in Siberia at 160 Ma, were also reported by Broadley et al. (2018a). However, the bulk halogen compositions of Obnazhennaya xenoliths are MORB- and OIB-like with significantly lower halogen concentrations, suggesting extensive halogen extraction and replenishment by the Siberian flood basalt magmatism at 250 Ma (Broadley et al., 2018a). Therefore the data for Obnazhennaya xenoliths are not suitable for comparison with kimberlites derived from SCLM, and not shown in figures in this paper.

The overall correlations among these halogen concentrations in the kimberlites indicate similar behaviors of the halogens during partial melting of the kimberlite source, and ascent and degassing of kimberlite magma. However, there is some scatter with the kimberlite data, which will be discussed in the following sections. The halogen concentrations in the kimberlite and xenolith samples vary over two or three orders of magnitude. The Siberian and Chinese kimberlites have markedly higher Cl and Br concentrations (>600 ppm and >10 ppm, respectively) than the other kimberlites, whereas I concentrations are in the same range as the others.

While MORB and OIB show relatively narrow ranges of Cl/Br (260–520) and

I/Br (0.009–0.054), variations of those ratios of the kimberlites (30–340 and 0.001–0.19, respectively) are larger. There is no systematic difference in kimberlite Cl/Br ratios depending on the sample localities (Fig. 1a). The xenoliths in South African and Siberian kimberlites including those reported by Broadley et al. (2018a) have similar Cl/Br ratios. On the other hand, in Fig. 1b, the kimberlites are geochemically and geographically grouped into two based on the I/Br ratios; namely, a high-I/Br (0.06–0.19) group (South Africa, Greenland, Canada, and Brazil) and a low-I/Br (0.001–0.010) group (China and Siberia). The I/Br ratio of xenolith in Greenland kimberlite is in the range of high-I/Br group. The I/Br ratios of xenoliths in Siberian kimberlites including those reported by Broadley et al. (2018a) are consistent with their host (low-I/Br group) except one sample (U-34/03) whose I/Br value is close to the high-I/Br group. The I/Br ratios of the high-I/Br group kimberlites and South African xenoliths are higher than those of MORB and OIB, whereas the low-I/Br group kimberlites and the most of Siberian xenoliths have lower I/Br ratios than MORB and OIB.

In Fig. 2, the I/Cl versus Br/Cl ratios are shown for the kimberlite samples and their xenoliths. The halogen compositions of high-I/Br group kimberlites (South Africa, Greenland, Canada, and Brazil) show a positive correlation between the I/Cl and Br/Cl starting from the area close to the MORB and OIB (Kendrick et al., 2017).

The pattern of low-I/Br group kimberlites from China and Siberia is similar to the evaporation trend of seawater (Zherebtsova and Volkova, 1966) but more enriched in I. Instead, it overlaps the area of the fluid phase in the seawater-altered oceanic crust (Chavrit et al., 2016) and fluid inclusions in the eclogites derived from the altered oceanic crust (Svensen et al., 2001) (Fig. 2). In the Siberian xenoliths analyzed in this study, one sample is classified into the high-I/Br group, and the other two are classified into the low-I/Br group. The peridotite xenoliths in the Udachnaya kimberlites reported by Broadley et al. (2018a), which belong to the low-I/Br group in Fig. 1b, are plotted close to the low-I/Br kimberlites and xenoliths in this study though their Br/Cl and I/Cl ratios are higher.

We compared the I/Br ratios and the Sr-Nd isotopic classification for the South African, the Greenland, and the Chinese kimberlite samples (see Table 1). The South African, the Greenland, and the Chinese samples have both Group I and Group II characteristics; whereas the former two are classified into the high-I/Br group in contrast to the Chinese samples, which are all classified into the low-I/Br group. There is no correlation between the two I/Br groups and the Sr-Nd isotopic groups.

This is the peer-reviewed, final accepted version for American Mineralogist, published by the Mineralogical Society of America.
The published version is subject to change. Cite as Authors (Year) Title. American Mineralogist, in press.
DOI: https://doi.org/10.2138/am-2021-7332. http://www.minsocam.org/

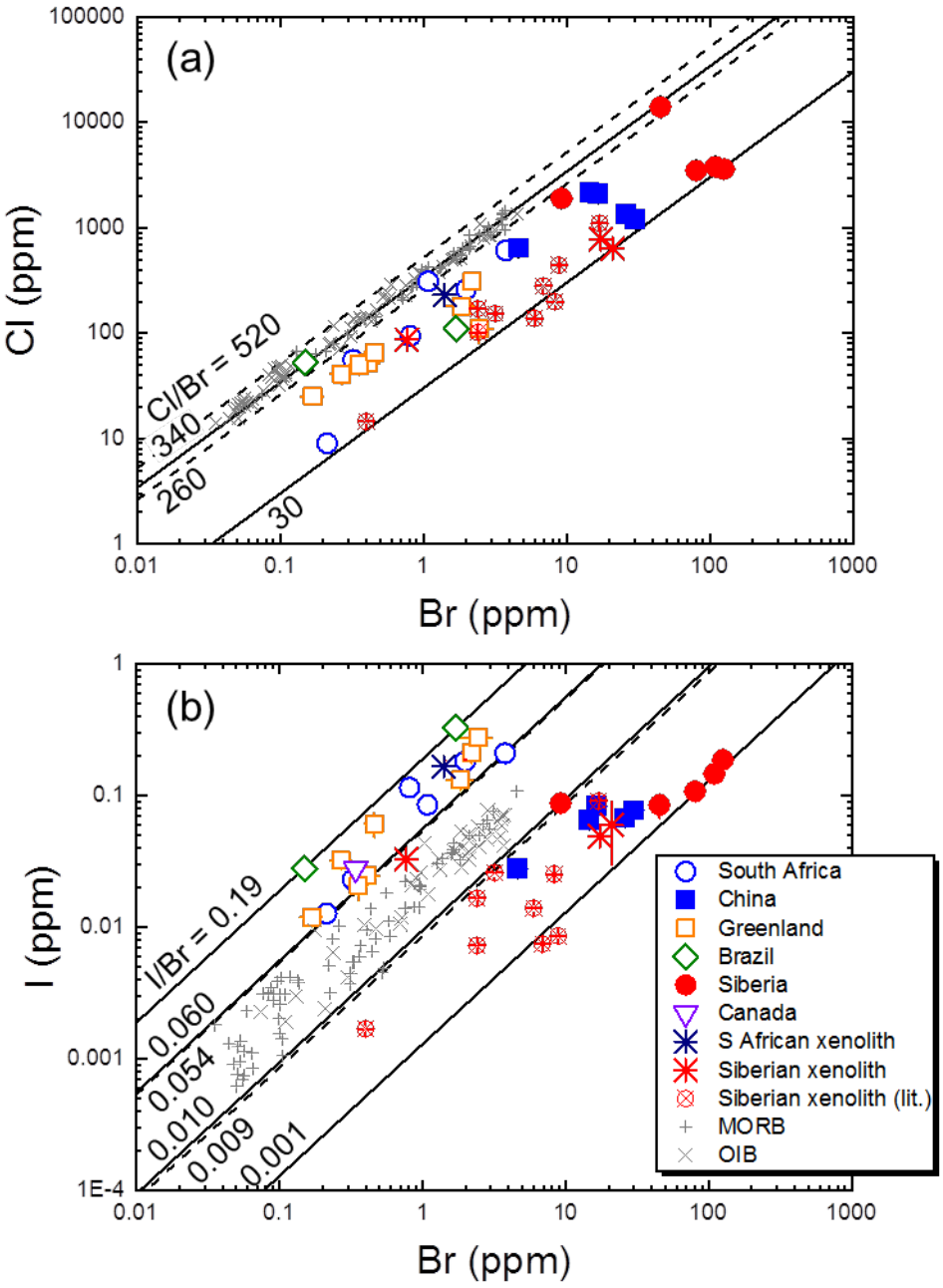

Fig. 1 Cl (a) and I (b) concentrations versus Br concentrations in kimberlite and xenolith samples. Data for peridotite xenoliths in Udachnaya kimberlite from Siberia reported by Broadley et al. (2018a) are also shown. Halogen concentrations of MORB and OIB are from Kendrick et al. (2017). The solid lines associated with numbers show

This is the peer-reviewed, final accepted version for American Mineralogist, published by the Mineralogical Society of America.
The published version is subject to change. Cite as Authors (Year) Title. American Mineralogist, in press.
DOI: https://doi.org/10.2138/am-2021-7332. http://www.minsocam.org/

maximum and minimum values of Cl/Br and I/Br ratios of kimberlites (in b, the values for high-I/Br and low-I/Br groups are shown) and broken lines are those for MORB and OIB. Error bars are one sigma, while most of them are smaller than the symbol size.

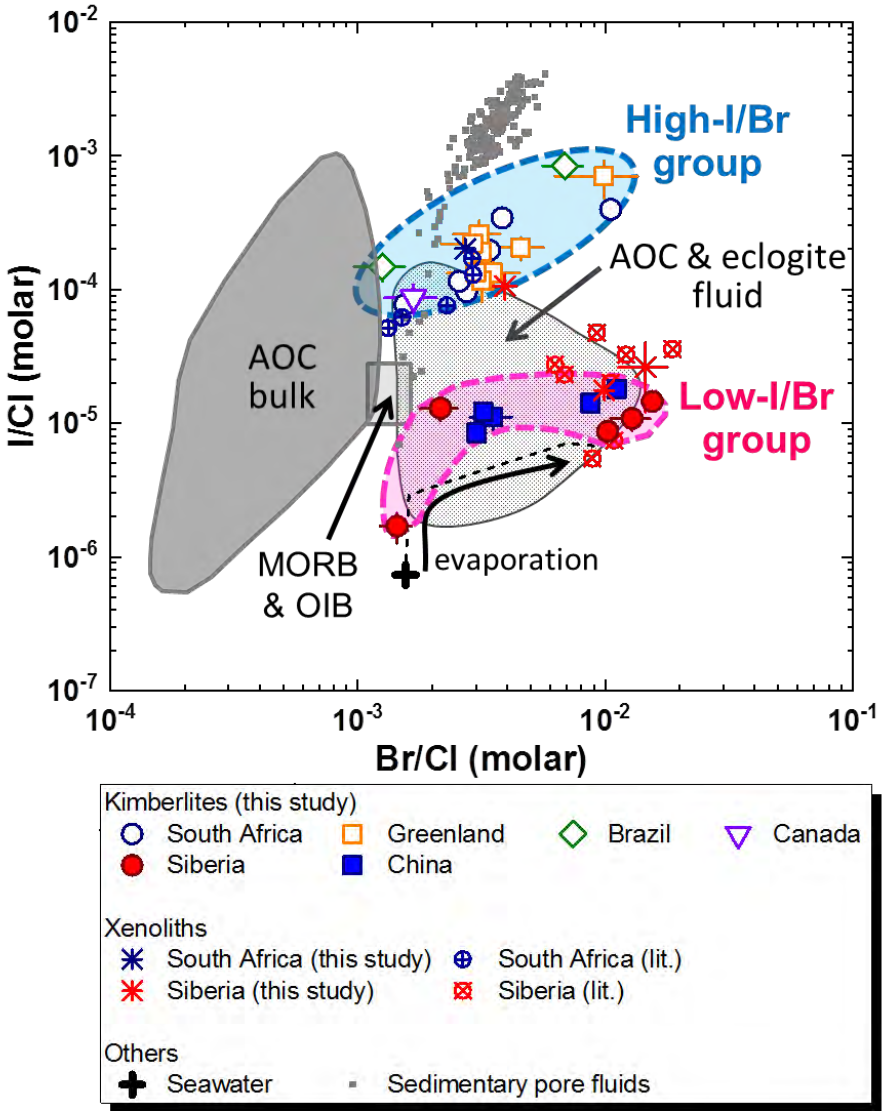

Fig. 2 I/Cl and Br/Cl ratios of kimberlites and their xenoliths from six localities (including the xenoliths in kimberlites from South Africa and Siberia by Johnson et al., 2000; Broadley et al., 2018a) compared with MORB, OIB (Kendrick et al., 2017), bulk compositions of altered oceanic crust (AOC, Chavrit et al., 2016), seawater (Riley and Skirrow, 1975), sedimentary pore fluids (Fehn et al., 2006), and fluids in AOC and eclogite (Chavrit et al., 2016; Svensen et al., 2001). The dashed line shows evaporation

trend of seawater from Zherebtsova and Volkova (1966). Error bars are one sigma.

5. Discussion

5.1. Possible modification of I/Br during/after magma ascent

The similarities and differences between the two kimberlite groups and other materials are keys to reveal the origin of the halogen signatures in each group.

Kamenetsky et al. (2004) reported that the Udachnaya kimberlites from Siberia are exceptionally fresh and show no secondary serpentinization. In fact, there is no visible alteration on the Siberian kimberlites used in this study (see photos of thin section in Supplementary Fig. 1). Sumino et al. (2006) separated fresh olivines and showed that the olivines still preserve mantle-derived noble gases, which are easy to overprint in olivines during alteration. In contrast, the Chinese kimberlites are not fresh. The olivines were almost entirely serpentinized, and the serpentinized olivines were altered to opaque minerals (i.e., the occurrence of fine-grained clay minerals) (Toyama et al., 2012) as shown in photos of thin section provided in Supplementary Fig. 1. The Siberian and Chinese kimberlites are quite different in terms of degree of alteration, but they show similar I/Br ratios nevertheless.

The effects of crustal contamination by the country rocks on the bulk rock composition must be considered because the kimberlites commonly entrain crustal xenoliths. The effects of crustal contamination (e.g., an increase in SiO_2, Al_2O_3, and Na_2O and a decrease in MgO and K_2O) can be quantified partially using the contamination index (C.I.), which is defined as the proportions of the clay minerals and the tectosilicates relative to the ferromagnesian minerals (olivine and phlogopite) given by Clement (1982). The C.I. values have been widely used to estimate the degree of crustal contamination on the kimberlite whole rock major oxide chemistry (e.g., Mitchell, 1976; Chalapathi Rao et al., 2004). The C.I. values of the kimberlites from South Africa and China were reported by Toyama et al. (2012). For the Greenland and the Siberian samples, we have calculated the C.I. from their major element compositions reported by Gaffney et al. (2007) and Kamenetsky et al. (2012). The kimberlites with C.I. < 1.4 are generally regarded as uncontaminated (Chalapathi Rao et al., 2004). The C.I. values of all the kimberlite samples in this study were < 1.4 and were not correlated with the group classified by the I/Br ratios (Fig. 3). This indicates that the apparent difference between the I/Br ratios of the two groups was likely not caused by crustal contamination.

Contamination of any evaporate (halite), which could be precipitated from

local waters, particularly saline brines, which carry halogens and interact with kimberlite during and after its emplacement (e.g., Stripp et al., 2006; Sader et al., 2007), would decrease the I/Cl ratio because evaporate halite with a low I/Cl has been reported (Zherebtsova and Volkova, 1966). In contrast, because the halogens in the kimberlite magma are concentrated in native halite crystals (Mass et al., 2005; Kamenetsky et al., 2004, 2012), the loss of the halite during alteration would elevate the I/Cl ratio of the bulk rock. Indeed, compared with the exceptionally fresh Udachnaya kimberlite, most kimberlites exhibit lower Cl and Na_2O contents. This might be due to the effect of halite removal during alteration (Kamenetsky et al., 2012). In order to evaluate the effect of halite contamination or removal on the halogen compositions of the bulk kimberlites, we investigated the correlation of the Na_2O with the I/Cl and the Br/Cl ratios in the kimberlites from South Africa and Greenland, for which the Na_2O data in South African and Greenland kimberlites are reported by Muramatsu (1983) and Gaffney et al. (2007) (see Fig. 4). However, we observed no clear correlation among them. The halogen concentrations of the Udachnaya kimberlite samples leached with de-ionized water are significantly lower by factors ranging 2–8 than the bulk samples (Table 1). However, the I/Cl and the Br/Cl ratios of the washed samples do not show significant change (Fig. 5). These lines of evidence, and the fact that the kimberlite samples investigated in this study are divided into two groups in terms of I/Br ratios, despite that they are from various locations where degree of interaction with local waters could vary locally, indicate that the contamination or removal of halite by local waters is not the principal cause of the variations in the halogen ratios of kimberlites.

Degassing of the kimberlite magma could be important for halogen fractionation, though experimental constraints for halogen behavior during degassing are quite limited. Fluid/melt partition coefficients of halogens decrease in the order of I > Br > Cl (Bureau et al., 2000), suggesting that degassing of the kimberlite magma engenders lower I/Br ratios associated with the low Br/Cl and I/Cl ratios in the degassed kimberlite magma. In the I/Cl versus Br/Cl diagram, the halogen composition of the degassed kimberlite should be shown in the lower left field. It is inconsistent with the observed trend in the I/Cl versus Br/Cl diagram for high-I/Br group kimberlites. Moreover, the initially low Br concentration in the high-I/Br group kimberlites cannot generate high Br in the low-I/Br group kimberlites by degassing.

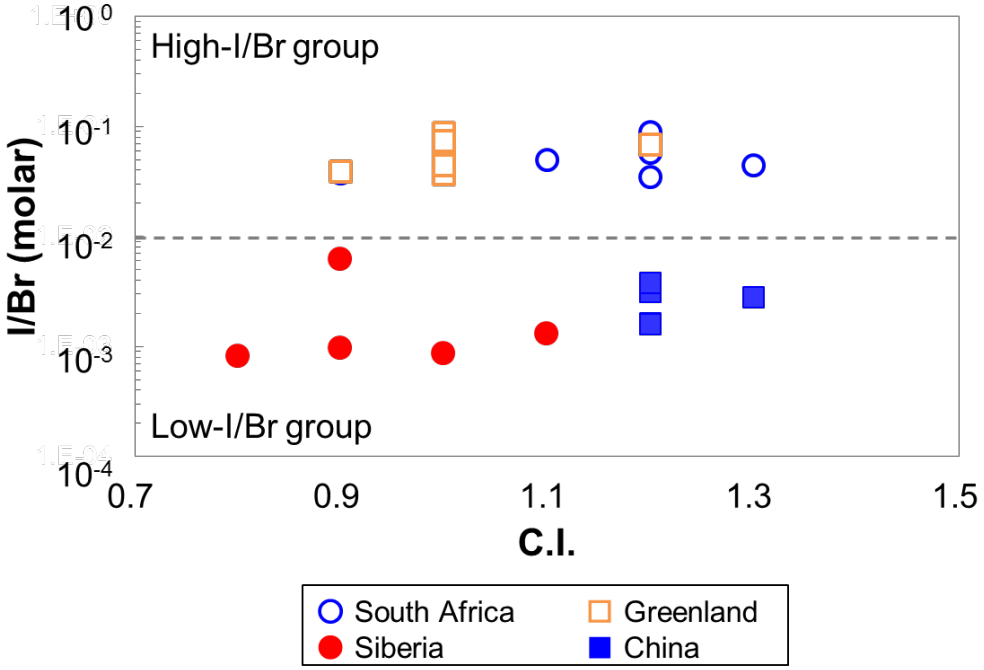

Fig. 3 The I/Br ratios and contamination index (C.I.) values of bulk rocks of kimberlites from South Africa, Greenland, China and Siberia. The C. I. values of kimberlites from South Africa and China were reported by Toyama et al. (2012). For the Greenland and Siberian samples, C.I. values were calculated using the major element compositions reported by Gaffney et al. (2007) and Kamenetsky et al. (2012), respectively.

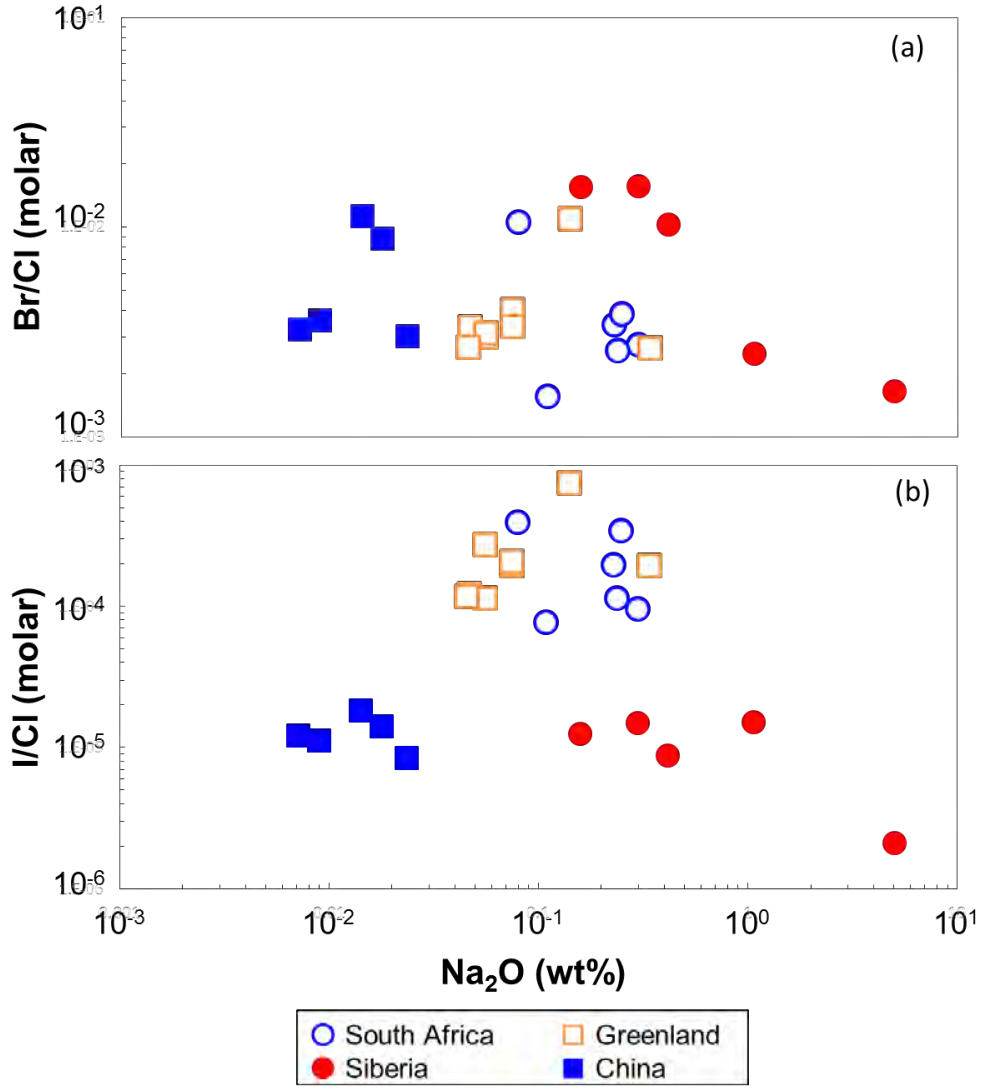

Fig. 4 Br/Cl and I/Cl ratios and Na_2O content of bulk rocks of kimberlites from South Africa, Greenland, China, and Siberia. Na_2O contents of kimberlites from South Africa and China were reported by Toyama et al. (2012). Those of Greenland and Siberian samples are from Gaffney et al. (2007) and Kamenetsky et al. (2012), respectively.

This is the peer-reviewed, final accepted version for American Mineralogist, published by the Mineralogical Society of America.
The published version is subject to change. Cite as Authors (Year) Title. American Mineralogist, in press.
DOI: https://doi.org/10.2138/am-2021-7332. http://www.minsocam.org/

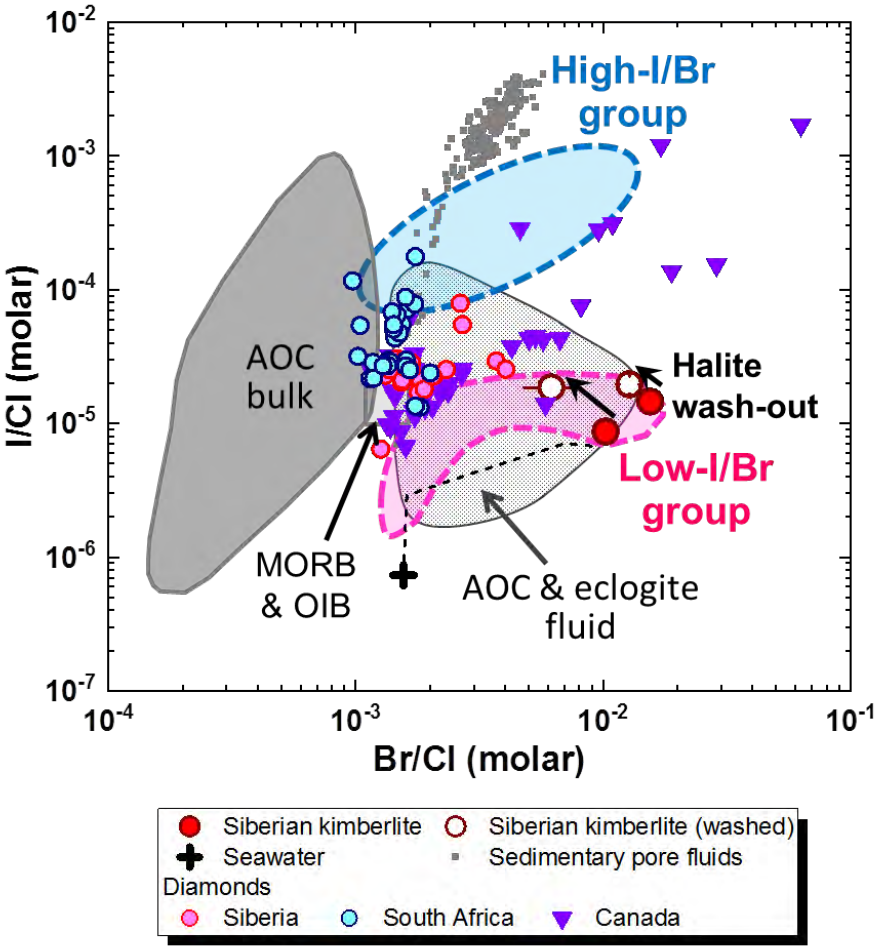

Fig. 5 Comparison of I/Cl and Br/Cl ratios of the bulk Siberian kimberlite and the residue after halite wash-out by water and those of diamonds from Siberia, South Africa, and Canada (Johnson et al., 2000; Burgess et al., 2002, 2009; Broadley et al., 2018b) with high-I/Br and low-I/Br kimberlite groups.

5.2. Origin of high-I/Br group kimberlites

The South African xenoliths analyzed in this study and those reported by Johnson et al. (2000) show halogen compositions similar to those of the South African kimberlites (Fig. 2). Assimilation of the SCLM with kimberlite magma during magma ascent might be responsible for the similarity. With an increase in the SiO_2 content of

the kimberlite magma, the degree of the SCLM assimilation increases (e.g., Russell et al., 2012). In Fig. 6a, the SiO_2 contents of the kimberlite samples from South Africa and Greenland are shown versus the Br/Cl ratios. There is no correlation, suggesting that the halogen compositions of the high-I/Br group kimberlites had not been modified during magma ascent through the lithosphere. Given that the incipient melt originated from the asthenosphere beneath SCLM had MORB- and OIB-like halogen composition (Kendrick et al., 2017), this suggests that the halogens in the melt would have overprinted by those in SCLM at the early stage of interaction, and halogen composition of SCLM of South Africa and Greenland would be homogeneous with depth. This is supported by the halogen compositions of some South African diamonds (Johnson et al., 2000; Burgess et al., 2002) plotted within the high-I/Br field (Fig. 5). In contrast, while the single data for Canadian kimberlite is plotted in the high-I/Br field, majority of diamonds from Canada (Johnson et al., 2000; Burgess et al., 2002; 2009) form a different trend having mantle-like I/Br ratio and a few samples are plotted in the low-I/Br field, suggesting the Canadian SCLM might be heterogeneous (Fig. 5). Since the high-I/Br component is also observed in a mantle xenolith from Siberia (Fig. 2), the high I/Br observed in the kimberlites from South Africa, Greenland, Canada and Brazil might be common nature of SCLM where the kimberlite magmas originated in and ascent through.

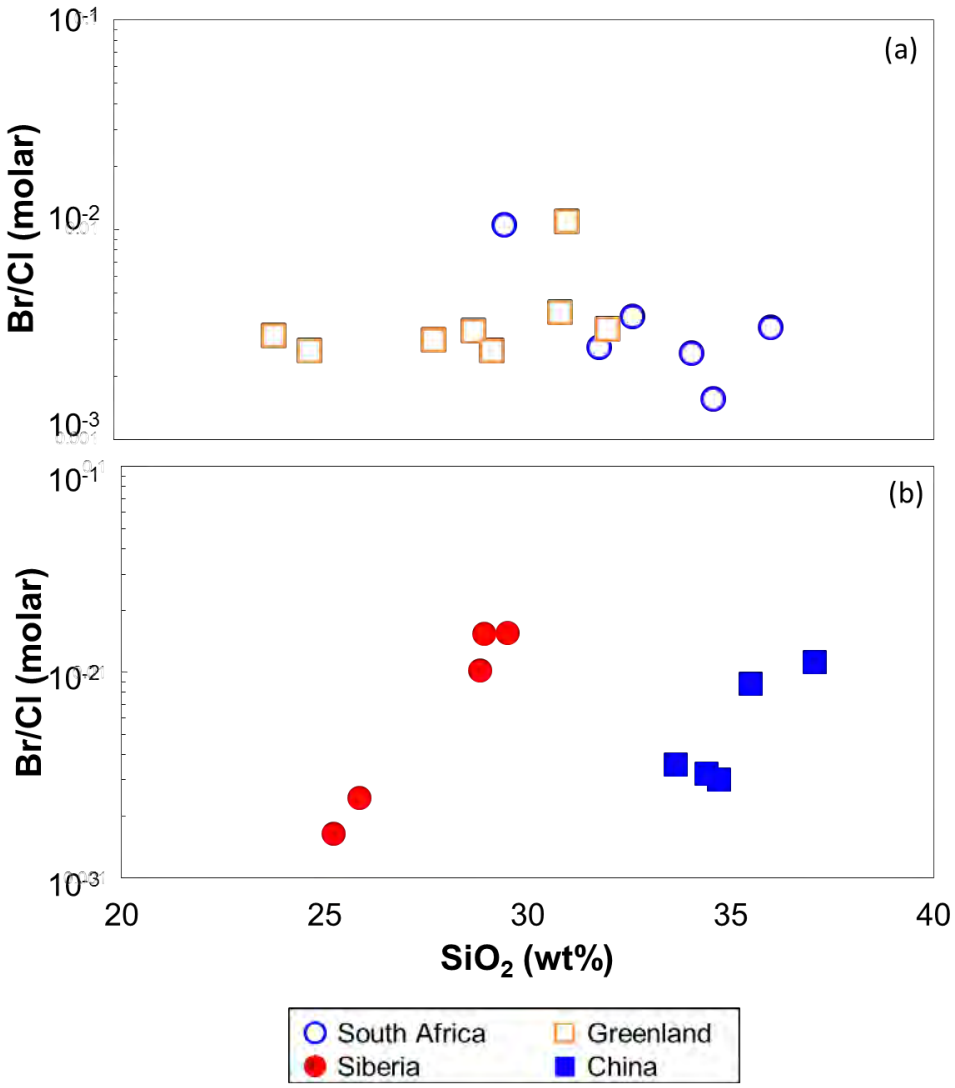

Fig. 6 Br/Cl ratio versus SiO_2 content of kimberlites from South Africa, Greenland, China, and Siberia. SiO_2 contents of kimberlites from South Africa and China were reported by Toyama et al. (2012). The Greenland and Siberian samples are from Gaffney et al. (2007) and Kamenetsky et al. (2012).

5.3. Origin of low-I/Br group kimberlites

The Siberian kimberlites are exceptionally fresh as indicated by the lack of serpentinization and the preservation of alkali carbonates and chlorides (Mass et al., 2005; Kamenetsky et al., 2004, 2012); while the Chinese kimberlites are severely altered as shown by the complete serpentinization of the olivine grains (Toyama et al.,

2012). Such results suggest that the low-I/Br is an intrinsic feature of the magma. Any effects, such as crustal contamination, degassing, and alteration, do not contribute the low-I/Br signature to the samples with high-Br signatures, as discussed above.

The halogen composition of a mantle xenolith in the Siberian kimberlite (a red asterisk in Fig. 2) is plotted in the high-I/Br field. Coexistence of both high-I/Br and low-I/Br characteristics in the low-I/Br group kimberlites (Siberia) suggests the involvement of at least two components. One is the high-I/Br component, which could be a common feature of SCLM. The other (the low-I/Br component) must be explained by some other processes. In this respect, it should be noted that the halogen compositions of the kimberlites from Siberia and China show values closer to fluids trapped within minerals in the altered oceanic crust or those trapped within eclogites (Fig. 2). This might indicate the possibility of the involvement of the seawater-derived or fractionated seawater-derived halogen in the kimberlite magma.

The mantle xenoliths from the Siberian kimberlites are classified into the two I/Br ratio groups. In addition, the Br/Cl ratios of Siberian and Chinese kimberlites increase as SiO_2 contents increase (Fig. 6b), suggesting that the halogen compositions of the primary magma of the low-I/Br group kimberlites were similar to those of the high-I/Br group kimberlites or MORB/OIB, while the SCLM would have been enriched in Br (i.e., low-I/Br) and might affect the primary kimberlite magma of deeper origin during its ascent to the surface (e.g., Russell et al., 2012).

Metasomatism is a pervasive process in the mantle, as exhibited by mantle xenoliths worldwide (e.g., Peason et al., 1995; Gaffney et al., 2007; Yang et al., 2009; Li et al., 2011). The SCLM beneath Siberia was reported to have been metasomatized by a carbonatitic melt, such as a kimberlite magma (e.g., Peason et al., 1995). However, as shown in the Br/Cl and SiO_2 relationship (Fig. 6b), the primary magma of the kimberlites would not exhibit halogen signatures similar to that of the seawater or the seawater-influenced eclogite. In addition, the halogen compositions of the OIBs from Samoa and Pitcairn, whose Nd-Sr-Pb isotope composition show association of subducted materials, are similar with that of the typical mantle (Kendrick et al., 2015; 2017). Hence the kimberlite magma would not originally have the halogen composition of the low-I/Br group, even if the magma source had been affected by subducted materials. Therefore, it is unlikely that the low I/Br signature of the SCLM beneath Siberia and China resulted from metasomatism by a kimberlite magma. The observations suggest that the halogen compositions in the low-I/Br group kimberlites were caused by the association with the SCLM, which would have partially changed into the low-I/Br group by the influence of the subducted seawater-derived halogens.

522

523 **5.4. Halogen composition of the kimberlite magma source**

524 The South African xenoliths and one Siberian xenolith are shown in the field of
525 the high-I/Br group kimberlite (Fig. 2), indicating that halogens with the high-I/Br
526 characteristics are common to those in SCLM and uniformly existed at least over
527 several hundred million years.

528 Broadley et al. (2018a) proposed that the Siberian flood basalt volcanism
529 extensively extracted halogens from the Siberian SCLM. The systematically lower Cl
530 and Br concentrations of the high-I/Br group kimberlites than those of the low-I/Br
531 group ones (Fig. 1a) could be accounted for by a similar process. However, the modified
532 halogen composition of SCLM after the flood basalt volcanism is similar to MORB and
533 OIB in the Siberian case (Broadley et al., 2018a), which is not consistent with the
534 observed halogen compositions of the high-I/Br group kimberlites. Therefore, halogen
535 extraction and replenishment by an extensive volcanism would not be responsible for
536 the halogen compositions of high-I/Br kimberlites and xenoliths.

537 Gaffney et al. (2007), Yang et al. (2009) and Li et al. (2011) proposed that the
538 source of the South African, Greenland, Siberian and Chinese kimberlite magmas was
539 affected by the ancient subducted oceanic crust because the kimberlites have distinctive
540 Hf isotope signatures. On the other hand, Woodhead et al. (2019) showed that the
541 kimberlites of western Canada, South Africa and Brazil are anomalous in Hf-Nd isotope
542 compositions compared to the global kimberlite data set and may have been influenced
543 by recent subduction, while kimberlites of Greenland, Siberia, China and northern
544 Canada (this study) may preserve pristine Hf-Nd isotopic compositions and have been
545 isolated from ancient subduction. In either case, therefore, there is a decoupling between
546 Hf (and Nd) isotopes and halogen systematics. Moreover, the halogen compositions of
547 the high-I/Br group kimberlites are not similar to those of the altered oceanic crust
548 (Chavrit et al., 2016) (Fig. 2). These suggest that the behavior of halogens is different
549 from that of Hf (and Nd) in a subducting slab.

550 Moreover, the I/Br ratios of the South African, Greenland, Brazilian, and
551 Canadian kimberlite samples used in our study are very similar to each other despite an
552 extremely low degree of the partial melting of the kimberlite incipient melt. This means
553 that the partition coefficients of Br and I between crystals and melts during the melting
554 process in the Earth's mantle would be almost the same at such high temperatures.

555 In contrast to the uniform I/Br ratio, the Br/Cl and I/Cl ratios of the high-I/Br
556 group kimberlites show a linear relationship (Fig. 2). Burgess et al. (2009) reported a
557 similar fractionation in Canadian diamonds, which is accounted for by Cl depletion

keeping mantle-like I/Br ratio, and concluded that it took place during the fluid–melt partitioning when forming silicic fluids during the separation of an immiscible saline fluid from the mixture. Therefore, if the mantle beneath South Africa, Greenland, Brazil, and Canada was metasomatized by such a fluid, it could have fractionated in terms of the Cl composition while preserving the original I/Br ratio, resulting in a positive fractionation trend as shown by the high-I/Br group kimberlites in Fig. 2. The original composition of the metasomatizing fluid (lower-left end of the trend formed by the high-I/Br group kimberlites in Fig. 2) exhibits higher I/Cl ratio than MORB and OIB, while Br/Cl is similar. As it is difficult to elevate I/Cl ratio without modifying Br/Cl ratio by any fractionation processes in the mantle, addition of another component enriched in I to the mantle is required. Sumino et al. (2010) and Kobayashi et al. (2017) reported that the halogens in the supra-subduction zone mantle are heavily enriched in I relative to Cl and Br due to addition of halogens originated from sedimentary pore fluids, which was carried by the serpentinites in the slab mantle. The pore fluids might have been intruded through bending-related faults in a subducting oceanic plate to form serpentinites (e.g., Faccenda et al., 2008). As serpentinites are strongly depleted in most incompatible trace elements (Kodolányi et al., 2012), its contribution would be hard to identify in Hf-Nd isotopic compositions of kimberlites. On the other hand, since serpentinite is able to contain relatively abundant halogens (up to 2300 ppm of I, Kendrick et al., 2013) and would survive to a great depth in subducting slab (van Keken et al., 2011), the involvement of serpentine-derived fluid may account for the high I/Cl ratio of metasomatizing fluid in SCLM.

The Siberian xenoliths suggest the involvement of the low-I/Br halogen component in SCLM. As discussed above, the I/Br ratio of the SCLM beneath Siberia and China would have been partly modified to a lower value by the influence of the subducted seawater-derived halogens. Since the halogen compositions of the low-I/Br group kimberlites are clearly distinct from the pore fluid compositions (Fig. 2), subducted halogens carried by the slab mantle serpentinite would not account for this component. As an alternate process for producing a high Br/Cl ratio in the SCLM, Kendrick et al. (2011) proposed that the dehydration of the serpentine beneath volcanic arcs engenders the elevated Br/Cl ratio of the residual olivine. However, this process does not lower the I/Cl ratio. Therefore, the sedimentary pore-fluid-derived halogen carried by serpentinites is unlikely as the source of the low-I/Br SCLM and, thus, the low-I/Br group kimberlites.

Alternatively, because hydrothermal alteration of the igneous oceanic crust and the serpentinite occurs at mid-ocean ridges that are affected by the seawater directly

without any sediment cover, the trapped fluids would have low I/Cl ratios and variable Br/Cl ratios as observed in seafloor serpentinites from modern mid-ocean ridge and passive margins (Kendrick et al., 2013). An observation that fluid phase trapped in altered oceanic crust has similar Br/Cl and I/Cl ratios to those in fluid inclusions trapped in eclogite (Chavrit et al., 2016) would indicate subduction of such halogens associated with oceanic crust. Therefore, the seawater-derived halogens observed in the low-I/Br group kimberlites and their mantle xenoliths may have been derived from such a subducted igneous oceanic crust and serpentinite hydrated by seawater at mid-ocean ridge without sedimentary-pore fluid contribution. Although we have no constraints for depths origin of our Siberian xenoliths associated with the low I/Br ratios, the low I/Br ratios are also identified in Siberian xenoliths derived from the basal lithosphere (Broadley et al., 2018a) and in Siberian diamonds derived from a depth greater than 150 km (Burgess et al., 2002; Broadley et al., 2018b), suggesting halogens with low I/Br would exist in a great depth in SCLM.

6. Implications

In order to reveal the characteristics of halogens in the mantle, we measured the concentrations of Cl, Br, and I in kimberlites and their xenoliths from South Africa, Greenland, Siberia, China, Canada, and Brazil. Based on the data obtained, the following conclusions can be derived:

1) The kimberlite samples and their xenoliths are classified into two groups with respect to their I/Br ratios (the high-I/Br and low-I/Br groups). Effects of alteration, crustal contamination, and degassing cannot explain the variation shown between the two kimberlite groups.
2) The Chinese and Siberian kimberlite samples show markedly lower I/Br ratios. Similarly low I/Br ratios have been observed in seawater-related materials such as the fluid inclusions in the eclogites derived from seawater-altered oceanic crust and in the seawater associated with halite precipitation.
3) It is inferred that the I/Br of SCLM would be relatively uniform with the high ratios.
4) There is a possibility that the SCLM beneath Siberia and China had the halogen composition of the high-I/Br group initially and might have partially changed into the low-I/Br group under the effect of the subducted seawater-derived halogens as reflected in the kimberlites of the low-I/Br group.

Broadley et al. (2018a) pointed out that halogen-rich SCLM affected by seawater-derived metasomatism would be an important reservoir in the Earth's halogen inventory. However, the results of this study imply that such role of SCLM is limited, since SCLM halogen compositions sampled by kimberlites from South Africa, Greenland, Canada and Brazil are characterized by systematically lower concentrations than those beneath Siberia and China by more than an order of magnitude, while degree of incipient melting in the kimberlite source region would not be vary so much (Fig. 1). Some of the halogen stored in SCLM beneath Siberia could be intensively extracted by Siberian Flood Basalt magmatism (Broadley et al., 2018a). On the other hand, no large igneous province magmatism has taken place in China, which implies seawater-derived halogens are still stored in SCLM beneath China with high concentrations. This hypothesis will be tested by analyzing halogens in alkaline basalt magmas erupted in China.

Acknowledgements.— This paper is dedicated to the memory of Y. Muramatsu (1950–2016) who was the pioneer of halogen analysis in geochemistry and a great mentor of C. Toyama and N. Okabe. J. Yamamoto and I. Kaneoka appreciate Y. Lai (Univ. Beijing), H. Kagi (Univ. Tokyo), and Y. Tachibana (Univ. Tokyo) for their help in collecting the Chinese kimberlites. We thank K.H. Wedepohl (Univ. Goettingen), A.M. Gaffney (Univ. Washington), M. Arima (Yokohama National Univ.), A. Motoki (State Univ. Rio de Janeiro), V. S. Kamenetsky and M. B. Kamenetsky (Univ. Tasmania), and A.L. Araujo and S.E. Sichel (LAGEMAR, UFF) for providing the kimberlite samples from South Africa, Greenland, Canada, Siberia and Brazil. We would like to thank J. Kimura (JAMSTEC), M. Broadley (CRPG, CNRS-Nancy), and R. Burgess (Univ. Manchester) for their useful comments and J. Hopp and an anonymous reviewer for constructive reviews. Handling of the paper with great patience by A. Cadoux is very much appreciated. This study was supported by the Japan Society for the Promotion of Science (JSPS) grants Grant-in-Aid for Young Scientists (B) No. 20740314 and Grant-in-Aid for Scientific Research (B) No. 23340169, and by the Sumitomo Foundation and Inamori Foundation, all conceded to H. Sumino.

References

Bebout, G.E. (1996) Volatile transfer and recycling at convergent margins:
mass-balance and insights from high-P/T metamorphic rocks. G.E. In Bebout,
D.W. Scholl, S.H. Kirby, J.P. Platt, Eds., Subduction Top to Bottom 179–193;

doi:10.1029/GM096p0179.

Becker, M., and le Roex, A.P. (2005) Geochemistry of South African On- and Off-craton, Group I and Group II Kimberlites: Petrogenesis and Source Region Evolution. Journal of Petrology 47, 673–703; doi:10.1093/petrology/egi089.

Bolfan-Casanova, N. (2005) Water in the Earth's mantle. Mineralogical Magazine 69, 229–257; doi:10.1180/0026461056930248.

Broadley, M.W., Ballentine, C.J., Chavrit, D., Dallai, L., and Burgess, R. (2016) Sedimentary halogens and noble gases within Western Antarctic xenoliths: Implications of extensive volatile recycling to the sub continental lithospheric mantle. Geochim. Cosmochim. Acta 176, 139-156: doi:10.1016/j.gca.2015.12.013.

Broadley, M.W., Barry, P.H., Ballentine, C.J., Taylor, L.A., and Burgess, R. (2018a) End-Permian extinction amplified by plume-induced release of recycled lithospheric volatiles. Nature Geoscience 11, 682-687.

Broadley, M.W., Kagi, H., Burgess, R., Zedgenizov, D., Mikhail, S., Almayrac, M., Ragozin, A., Pomazansky, B., and Sumino, H. (2018b) Plume-lithosphere interaction, and the formation of fibrous diamonds. Geochemical Perspectives Letters 8, 26–30; doi:10.7185/geochemlet.1825.

Bureau, H., Keppler, H., and Metrich, N. (2000) Volcanic degassing of bromine and iodine: experimental fluid/melt partitioning data and applications to stratospheric chemistry. Earth Planet. Sci. Lett. 183, 51–60; doi:10.1016/S0012-821X(00)00258-2.

Burgess, R., Layzelle, E., Turner, G., and Harris, J.W. (2002) Constraints on the age and halogen composition of mantle fluids in Siberian coated diamonds. Earth and Planetary Science Letters, 197, 193-203.

Burgess, R., Cartigny, P., Harrison, D., Hobson, E., and Harris, J. (2009) Volatile composition of microinclusions in diamonds from the Panda kimberlite, Canada: Implications for chemical and isotopic heterogeneity in the mantle. Geochim. Cosmochim. Acta 73, 1865–1891; doi:10.1016/j.gca.2008.12.025.

Chalapathi Rao, N., Gibson, S., Pyle, D., and Dickin, A. (2004) Petrogenesis of Proterozoic lamproites and kimberlites from the Cuddapah basin and Dharwar craton, southern India. J. Petrol. 45, 907–948; doi:10.1093/petrology/egg116.

Chavrit, D., Burgess, R., Sumino, H., Teagle, D.A.H., Droop, G., Shimizu, A., and Ballentine, C.J. (2016) The contribution of the hydrothermal alteration of the ocean crust on the deep halogen and noble gas cycles. Geochimi Cosmochimi Acta, 183, 106-124..

Clement, C.R. (1982) A comparative geological study of some major kimberlite pipes in the Northern Cape and Orange Free State. Ph.D. thesis, University of Cape Town.

Déruelle, B., Dreibus, G., and Jambon A. (1992) Iodine abundances in oceanic basalts: implications for Earth dynamics. Earth Planet. Sci. Lett. 108, 217–227; doi:10.1016/0012-821X(92)90024-P.

Dobbs, P.N., Duncan, D.J., Hu, S., Shee, S.R., Colgan, E., Brown, M.A., Smith, C.B., and Allsopp, H.L. (1994) The geology of the Mengyin kimberlites, Shandong, China. Kimberlites, Related Rocks and Mantle Xenoliths. Proc. Int. Kimb. Conf., 5th, Araxá, Brazil, (Leonardos, O.H., and Meyer, H.O.A. eds.), 1, 40–61.

Faccenda, M., Burlini, L., Gerya, T.V., and Mainprice, D. (2008) Fault-induced seismic anisotropy by hydration in subducting oceanic plates. Nature 455, 1097–1100; doi:10.1038/nature07376.

Fehn, U., Lu, Z., and Tomaru, H. (2006) Data report: ^{129}I/I ratios and halogen concentrations in pore water of Hydrate Ridge and their relevance for the origin of gas hydrates: a progress report, In: Trehu, A.M., Bohrmann, G., Torres, M.E., Colwell, F.S., Eds., Proceedings of the Ocean Drilling Program, Scientific Results Volume 204. Ocean Drilling Program, College Station, TX, pp. 1-25.

Gaffney, A.M., Blichert-Toft, J., Nelson, B.K., Bizzarro, M., Rosing, M., and Albarède, F. (2007) Constraints on source-forming processes of West Greenland kimberlites inferred from Hf–Nd isotope systematics. Geochim. Cosmochim. Acta 71, 2820–2836; doi:10.1016/j.gca.2007.03.009.

Holland, G., and Ballentine, C.J. (2006) Seawater subduction controls the heavy noble gas com-position of the mantle. Nature 441, 186–191; doi:10.1038/nature04761.

Jambon, A., Dérulle, B., Dreibus, G., and Pineau, F. (1995) Chlorine and Bromine abundances in MORB: the contrasting behavior of the Mid- Atlantic Ridge and East Pacific Rise and implications for Chlorine geodynamic cycle. Chem. Geol. 126, 101–117; doi:10.1016/0009-2541(95)00112-4.

Jarrard, R.D. (2003) Subduction fluxes of water, carbon dioxide, chlorine, and potassium. Geochem. Geophys. Geosyst. 4, 8905; doi:10.1029/2002GC000392.

Johnson, L.H., Burgess, R., Turner, G., Milledge, H.J., and Harris, J.W. (2000) Noble gas and halogen geochemistry of mantle fluids: comparison of African and Canadian diamonds. Geochim. Cosmochim. Acta 64, 717–732; doi:10.1016/S0016-7037(99)00336-1.

Kamenetsky, M.B., Sobolev, A.V., Kamenetsky, V.S., Mass, R., Danyushevsky, L.V., Thomas, R., Pokhilenko, N.P., and Sobolev, N.V. (2004) Kimberlite melts rich in

alkali chlorides and carbonates: A potent metasomatic agent in the mantle. Geology 32, 845–848; doi:10.1130/G20821.1.

Kamenetsky, V.S., Kamenetsky, M.B., Golovin, A.V., Sharygin, V.V., and Maas, R. (2012) Ultrafresh salty kimberlite of the Udachnaya–East pipe (Yakutia, Russia): A petrological oddity or fortuitous discovery? Lithos 152, 173–186; doi:10.1016/j.lithos.2012.04.032.

Kendrick, M.A., Scambelluri, M., Honda, M., and Phillips, D. (2011) High abundances of noble gas and chlorine delivered to the mantle by serpentinite subduction. Nature Geoscience 4, 807–812; doi:10.1038/ngeo1270.

Kendrick, M. A., Kamenetsky, V.S., Phillips, D., and Honda, M. (2012) Halogen systematics (Cl, Br, I) in Mid-Ocean Ridge Basalts: A Macquarie Island case study. Geochim. Cosmochim. Acta 81, 82–93; doi:10.1016/j.gca.2011.12.004.

Kendrick, M. A., Honda, M., Pettke, T., Scambelluri, M., Phillips, D., and Giuliani, A. (2013) Subduction zone fluxes of halogens and noble gases in seafloor and forearc serpentinites. Earth Planet. Sci. Lett. 365, 86–96; doi:10.1016/j.epsl.2013.01.006.

Kendrick, M. A., Jackson, M.G., Hauri, E.H., and Phillips, D. (2015) The halogen (F, Cl, Br, I) and H_2O systematics of Samoan lavas: Assimilated-seawater, EM2 and high-$^3He/^4He$ components. Earth Planet. Sci. Lett. 410, 197–209; doi: 10.1016/j.epsl.2014.11.026.

Kendrick, M.A., Hemond, C., Kamenetsky, V.S., Danyushevsky, L., Devey, C.W., Rodemann, T., Jackson, M.G., and Perfit, M.R. (2017) Seawater cycled throughout Earth's mantle in partially serpentinized lithosphere. Nature Geosci 10, 222-228.

Kobayashi, M., Sumino, H., Nagao, K., Ishimaru, S., Arai, S., Yoshikawa, M., Kawamoto, T., Kumagai, Y., Kobayashi, T., Burgess, R., and Ballentine, C.J., (2017) Slab-derived halogens and noble gases illuminate closed system processes controlling volatile element transport into the mantle wedge. Earth Planet. Sci. Lett. 457, 106-116.

Kodolányi, J., Pettke, T., Spandler, C., Kamber, B.S., and Gméling, K. (2012) Geochemistry of Ocean Floor and Fore-arc Serpentinites: Constraints on the Ultramafic Input to Subduction Zones. Journal of Petrology, 53, 235-270.

Korotev, R.L. (1996) A Self-Consistent Compilation of Elemental Concentration Data for 93 Geochemical Reference Samples. Geost. Newsletter 20, 217–245; doi:10.1111/j.1751-908X.

Kramers, J.D., and Smith, C.B. (1983) A feasibility study of U−Pb and Pb−Pb dating of

kimberlites using groundmass mineral fractions and whole-rock samples. Chem. Geol. 41, 23–38; doi:10.1016/S0009-2541(83)80003-5.

Li, Q.L., Wu, F.Y., Li, X.H., Qiu, Z.L., Liu, Y., Yang, Y.H., and Tang, G.Q. (2011) Precisely dating Paleozoic kimberlites in the North China Craton and Hf isotopic constraints on the evolution of the subcontinental lithospheric mantle. Lithos 126, 127–134; doi:10.1016/j.lithos.2011.07.001.

Lu, F., Zheng, J., Zhao, L., Xia, W., and Zhang, H. (1995) Palaeozoic lithospheric mantle composition and processes beneath North China Platform (Extended Abstract). Int. Kimb. Conf., 6th, Novosibirsk, Russia, 336–338.

Mass, R., Kamenetsky, M.B., Sobolev, A.V., Kamenetsky, V.S., and Sobolev, N.V. (2005) Sr, Nd, and Pb isotope evidence for a mantle origin of alkali chlorides and carbonetes in the Udachnaya kimberlite, Siberia. Geology 33, 549–552; doi:10.1130/G21257.1.

Meyer, H.O.A., Garwood, B.L., Svicero, D.P., and Smith, C.B. (1994) Alkaline intrusions in western Minas Gerais, Brazil. Proc. Int. Kimb. Conf., 5th, Araxá, Brazil, (Leonardos, O.H., and Meyer, H.O.A. eds.), 1, 140–155.

Mirnejad, H., and Bell, K. (2006) Origin and Source Evolution of the Leucite Hills Lamproites: Evidence from Sr–Nd–Pb–O Isotopic Compositions. Journal of Petrology 47, 2463–2489; doi:10.1093/petrology/egl051.

Mitchell, R.H. (1976) Kimberlites of Somerset Island, District of Franklin. Geological Survey of Canada, 76-1A, 501–502.

Mitchell, R.H. (2012) Kimberlites, orangeites, and related rocks. Springer Science & Business Media, 410 pp.

Mitchell, R.H., and Meyer, H.O.A. (1980) Mineralogy of micaceous kimberlites from the Jos dyke, Somerset Island, N.W.T. Canadian Mineralogist 18, 241–250.

Muramatsu, Y. (1983) Geochemical investigations of kimberlites from the Kimberley area, South Africa. Geochem. J. 17, 71–86; doi:10.2343/geochemj.17.71.

Muramatsu, Y., and Wedepohl, K.H. (1985) REE and selected trace elements in kimberlites from the Kimberley are (South Africa). Chem. Geol. 51, 289–301; doi:10.1016/0009-2541(85)90138-X.

Muramatsu, Y., and Wedepohl, K.H. (1998) The distribution of iodine in the earth's crust. Chem. Geol. 147, 201–216; doi:10.1016/S0009-2541(98)00013-8.

Peason, D.G., Shirey, S.B., Carlson, R.W., Boyd, F.R., Pokhilenko, N.P., and Shimizu, N. (1995) Re-Os, Sm-Nd, and Rb-Sr isotope evidence for thick Archaean lithospheric mantle beneath the Siberian craton modified by multistage metasomatism. Geochim. Cosmochim. Acta 59, 959–977;

doi:10.1016/0016-7037(95)00014-3.

Pearson, D.G., Woodhead, J., and Janney, P.E. (2019) Kimberlites as Geochemical Probes of Earth's Mantle. Elements 15, 387–392; doi:10.2138/gselements.15.6.387.

Riley, J.P., and Skirrow, G. (1975) Chemical Oceanography. Academic Press 4, 2nd Edition.

Ringwood, A., Kesson, S., Hibberson, W., and Ware, N. (1992) Origin of kimberlites and related magmas. Earth Planet. Sci. Lett. 113, 521–538; doi:10.1016/0012-821X(92)90129-J.

Russell, J.K., Porritt, L.A., Lavallée, Y., and Dingwell, D.B. (2012) Kimberlite ascent by assimilation-fuelled buoyancy. Nature 481, 352–356; doi:10.1038/nature10740.

Sader, J.A., Leybourne, M.I., McClenaghan, M.B., and Hamilton, S.M. (2007) Low-temperature serpentinization processes and kimberlite groundwater signatures in the Kirkland Lake and Lake Timiskiming kimberlite fields, Ontario, Canada: implications for diamond exploration. Geochemistry: Exploration, Environment, Analysis, 7, 3-21.

Seno, T. (2009) Determination of the pore fluid pressure ratio at seismogenic megathrusts in subduction zones: Implications for strength of asperities and Andean-type mountain building. J. Geophys. Res. 114, B5; doi:10.1029/2008JB005889.

Shinonaga, T., Ebihara, M., Nakahara, H., Tomura, K., and Heumann, K.G. (1994) Cl, Br and I in igneous standard rocks. Chem. Geol. 115, 213–225; doi:10.1016/0009-2541(94)90187-2.

Smith, C.B. (1983) Pb, Sr and Nd isotopic evidence for sources of southern African Cretaceous kimberlites. Nature 304, 51–54; doi:10.1038/304051a0.

Sparks, R.S.J. (2013) Kimberlite volcanism. Annual Review of Earth Planet. Sci. 41, 497–528; doi:10.1146/annurev-earth-042711-105252.

Stripp, G.R., Field, M., Schumacher, J.C., Sparks, R.S.J., and Cressey, G. (2006) Post-emplacement serpentinization and related hydrothermal metamorphism in a kimberlite from Venetia, South Africa. Journal of Metamorphic Geology, 24, 515-534.. doi:10.1111/j.1525-1314.2006.00652.x.

Sumino, H., Kaneoka, I., Matsufuji, K., and Sobolev, A.V. (2006) Deep mantle origin of kimberlite magmas revealed by neon isotopes. Geophys. Res. Let. 33, L16318; doi:10.1029/2006GL027144.

Sumino, H., Burgess, R., Mizukami, T., Wallis, S.R., Holland, G., and Ballentine, C.J.

(2010) Seawater-derived noble gases and halogens preserved in exhumed mantle wedge peridotite. Earth Planet. Sci. Lett. 294, 163–172; doi:10.1016/j.epsl.2010.03.029.

Svensen, H., Jamtveit, B., Banks, D.A., and Austrheim, H. (2001) Halogen contents of eclogite facies fluid inclusions and minerals: Caledonides, western Norway. J. metamorphic Geology 19, 165–178; doi:10.1046/j.0263-4929.2000.00301.x.

Tachibana, Y., Kaneoka, I., Gaffney, A., and Upton, B. (2006) The ocean-island basalt-like source of kimberlite magmas from West Greenland revealed by high $^{3}He/^{4}He$ ratios. Geology 34, 273–276; doi:10.1130/G22201.1.

Toyama, C., Muramatsu, Y., Yamamoto, J., Nakai, S., and Kaneoka, I. (2012) Sr and Nd isotope ratios and trace element concentrations in kimberlites from Shandong and Liaoning (China) and the Kimberley area (South Africa). Geochem. J. 46, 45–59; doi:10.2343/geochemj.1.0151.

Torsvik, T., Burke, K., Steinberger, B., Webb, S., and Ashwal, L. (2010) Diamonds sampled by plumes from the core-mantle boundary. Nature 466, 352–355; doi:10.1038/nature09216.

Ulmer, P. (2001) Partial melting in the mantle wedge — the role of H_2O in the genesis of mantle-derived 'arc-related' magmas. Physics of the Earth and Planetary Interiors 127, 215–232; doi:10.1016/S0031-9201(01)00229-1.

van Keken, P.E., Hacker, B.R., Syracuse, E.M., and Abers, G.A. (2011) Subduction factory: 4. Depth-dependent flux of H_2O from subducting slabs worldwide. Journal of Geophysical Research, 116, B01401, doi:10.1029/2010JB007922.

Woodhead, J., Hergt, J., Giuliani, A., Maas, R., Phillips, D., Pearson, D.G., and Nowell, G. (2019) Kimberlites reveal 2.5-billion-year evolution of a deep, isolated mantle reservoir. Nature 573, 578–581; doi:10.1038/s41586-019-1574-8.

Wu, F., Yang, Y.H., Mitchell, R.H., Li, Q.L., Yang, J.H., and Zhang, Y.B. (2010) In situ U–Pb age determination and Nd isotopic analysis of perovskites from kimberlites in southern Africa and Somerset Island, Canada. Lithos 115, 205–222; doi:10.1016/j.lithos.2009.12.010.

Yang, Y.H., Wu, F.Y., Wilde, S.A., Liu, X.M., Zhang, Y.B., Xie, L.W., and Yang, J.H. (2009) In situ perovskite Sr–Nd isotopic constraints on the petrogenesis of the Ordovician Mengyin kimberlites in the North China Craton. Chem. Geol. 264, 24–42; doi:10.1016/j.chemgeo.2009.02.011.

Zherebtsova, I.K., and Volkova, N.N. (1966) Experimental study of behavior of trace elements in the process of natural solar evaporation of Black Sea and Sasyk-Sivash Brine. Geochemistry international 3, 656–670.

882

This is the peer-reviewed, final accepted version for American Mineralogist, published by the Mineralogical Society of America.
The published version is subject to change. Cite as Authors (Year) Title. American Mineralogist, in press.
DOI: https://doi.org/10.2138/am-2021-7332. http://www.minsocam.org/

883 **Table 1** Halogen compositions of kimberlite and xenolith samples.

	Area	Sample No.	Cl (ppm)			Br (ppm)			I (ppm)			I/Br ratio			Isotopic Group**
Bulk	South Africa*	K-1	260*			2.0*			0.18*			0.092*			II
		K-2	9*			0.21*			0.013			0.060*			I
		K-4	94*			0.81*			0.12*			0.14*			I
		K-6	610*			3.8*			0.21*			0.056*			I
		K-7	310*			1.1*			0.085*			0.079*			I
		K-8	56*			0.32*			0.023*			0.071*			I
	China	L-3	1200	±	100	30.1	±	0.6	0.077	±	0.003	0.00257	±	0.00012	T
		L-4	1330	±	8	26.1	±	0.7	0.067	±	0.003	0.00257	±	0.00014	T
		SH-1	2150	±	20	14.6	±	0.3	0.0649	±	0.0003	0.00444	±	0.00009	I
		SH-3	2100	±	400	16.6	±	0.3	0.083	±	0.0010	0.00502	±	0.00010	I
		SH-5	640	±	10	4.6	±	0.3	0.028	±	0.0013	0.0060	±	0.0005	I
	Greenland	Kim-1	52	±	10	0.41	±	0.09	0.025	±	0.004	0.06	±	0.02	I
		Kim-2	180	±	20	1.8	±	0.4	0.13	±	0.02	0.07	±	0.02	I
		Kim-7	310	±	30	2.2	±	0.3	0.21	±	0.03	0.10	±	0.02	I
		Kim-9	50	±	10	0.36	±	0.05	0.021	±	0.005	0.06	±	0.02	I
		Kim-11	110	±	30	2.4	±	0.6	0.28	±	0.04	0.11	±	0.03	I
		Kim-12	66	±	10	0.46	±	0.07	0.061	±	0.013	0.13	±	0.03	I
		Kim-13	41	±	8	0.27	±	0.05	0.032	±	0.004	0.12	±	0.03	I
		Kim-14	25	±	4	0.17	±	0.03	0.0120	±	0.0009	0.071	±	0.014	I
	Brazil	X-218	53	±	10	0.15	±	0.02	0.028	±	0.003	0.19	±	0.03	

This is the peer-reviewed, final accepted version for American Mineralogist, published by the Mineralogical Society of America.
The published version is subject to change. Cite as Authors (Year) Title. American Mineralogist, in press.
DOI: https://doi.org/10.2138/am-2021-7332. http://www.minsocam.org/

		X-219	110	±	10	1.7	±	0.3	0.33	±	0.02	0.19	±	0.03
	Siberia	K1/05	3600	±	100	125.6	±	0.7	0.187	±	0.009	0.00149	±	0.00007
		YBK-2	3490	±	40	80.5	±	0.9	0.108	±	0.008	0.00137	±	0.00010
		YBK-3	14000	±	2000	45.4	±	0.8	0.09	±	0.02	0.0019	±	0.0004
		K6/04	3800	±	600	110	±	10	0.147	±	0.015	0.0013	±	0.0002
		K24/04	1900	±	300	9.2	±	0.6	0.088	±	0.009	0.0095	±	0.0011
	Canada	C-1	90	±	20	0.34	±	0.03	0.028	±	0.003	0.082	±	0.003
Water leached	Siberia	K1/05	1100	±	100	31.7	±	0.6	0.077	±	0.009	0.0024	±	0.0003
		YBK-2	770	±	160	10.7	±	0.9	0.051	±	0.008	0.0048	±	0.0008
Xenolith	South Africa	GP-14	230*			1.41	±	0.06	0.166	±	0.003	0.118	±	0.006
	Russia	U-12/05	640	±	130	21	±	2	0.06	±	0.03	0.0029	±	0.0015
		U-34/03	87	±	9	0.77	±	0.04	0.033	±	0.006	0.043	±	0.008
		U-01/04	780	±	20	17.4	±	0.6	0.049	±	0.003	0.0028	±	0.0002

Errors are standard deviation of repeated analyses (n = 2–5). *No error was estimated because only a single analysis was made. **Grouped based on Nd-Sr isotopic compositions by Gaffney et al. (2007) and Toyama et al. (2012).

This is the peer-reviewed, final accepted version for American Mineralogist, published by the Mineralogical Society of America.
The published version is subject to change. Cite as Authors (Year) Title. American Mineralogist, in press.
DOI: https://doi.org/10.2138/am-2021-7332. http://www.minsocam.org/

Fig. 1

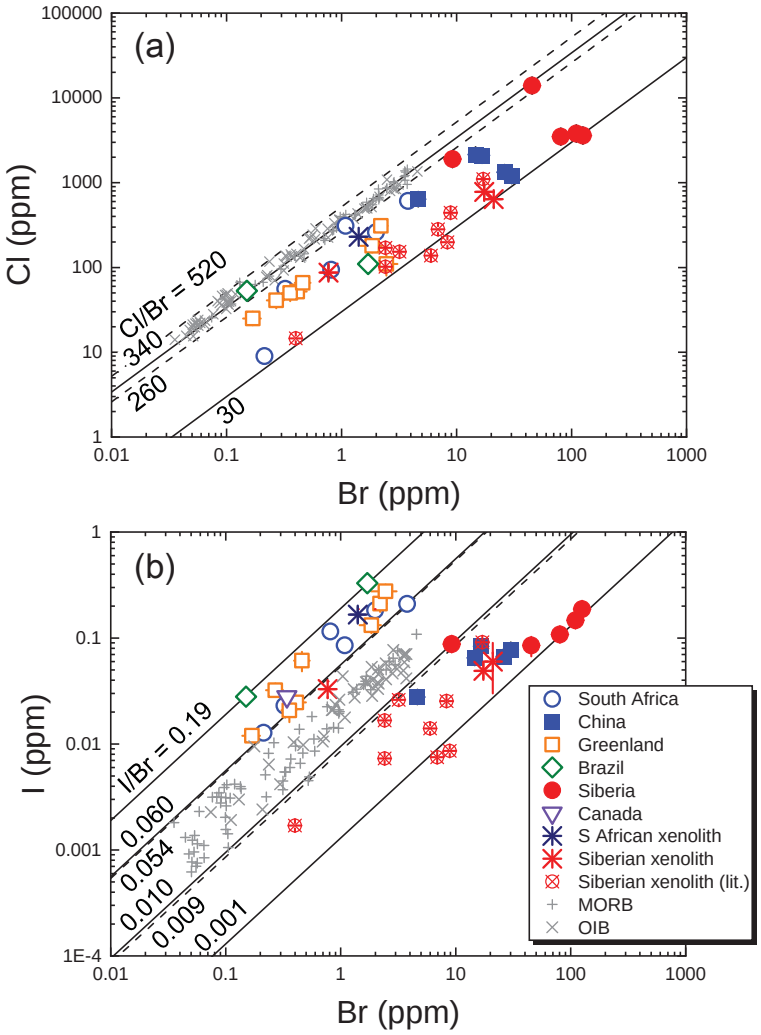

This is the peer-reviewed, final accepted version for American Mineralogist, published by the Mineralogical Society of America.
The published version is subject to change. Cite as Authors (Year) Title. American Mineralogist, in press.
DOI: https://doi.org/10.2138/am-2021-7332. http://www.minsocam.org/

Fig. 2

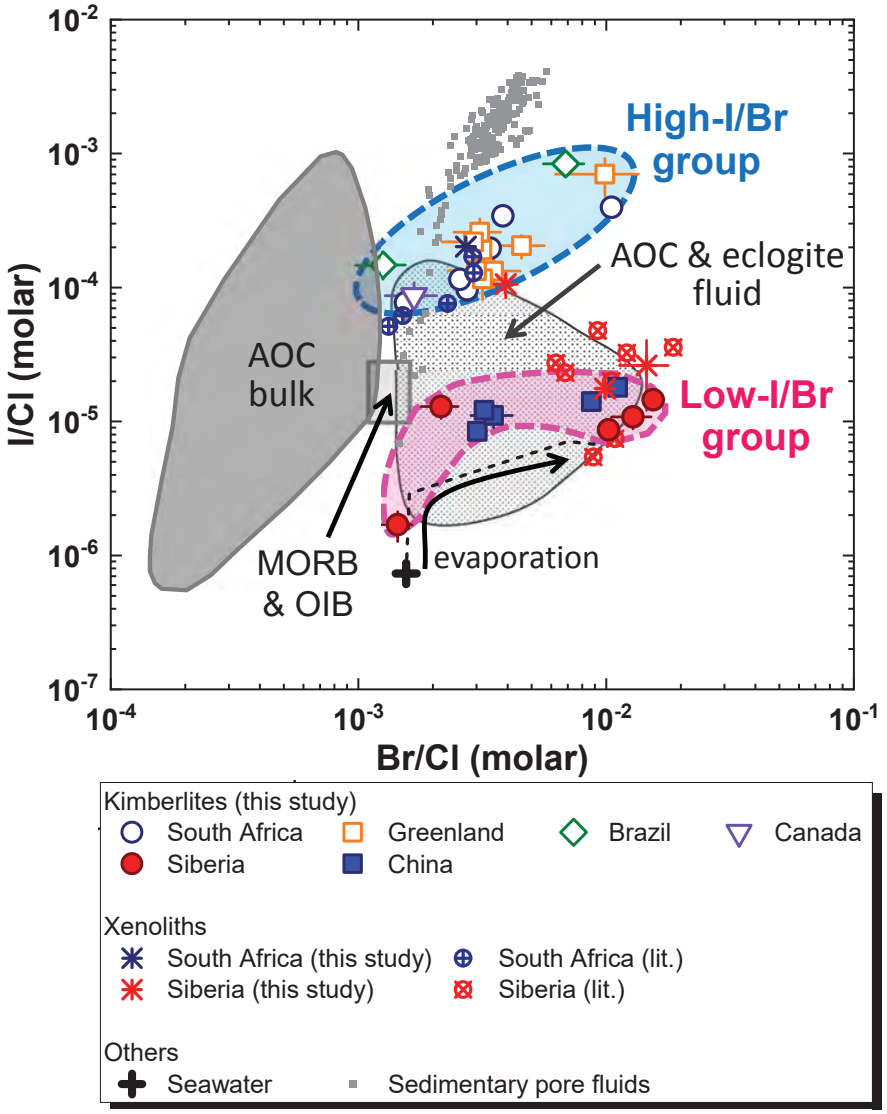

Fig.3

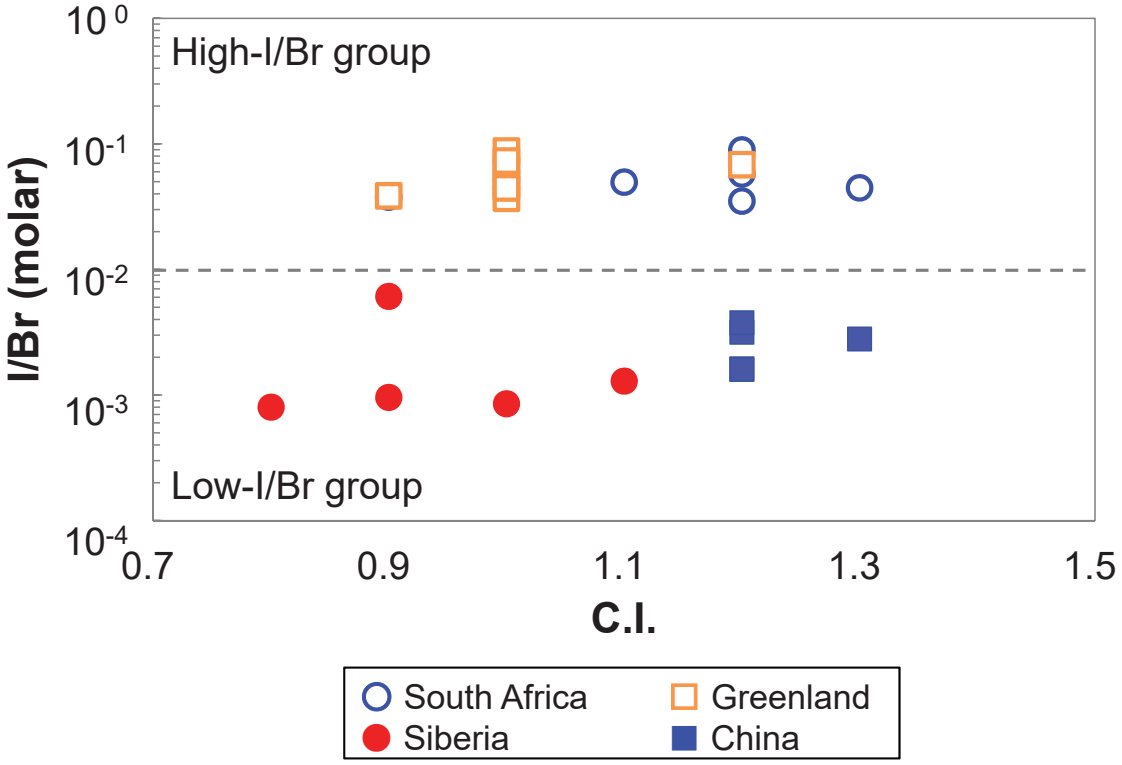

This is the peer-reviewed, final accepted version for American Mineralogist, published by the Mineralogical Society of America.
The published version is subject to change. Cite as Authors (Year) Title. American Mineralogist, in press.
DOI: https://doi.org/10.2138/am-2021-7332. http://www.minsocam.org/

Fig.4

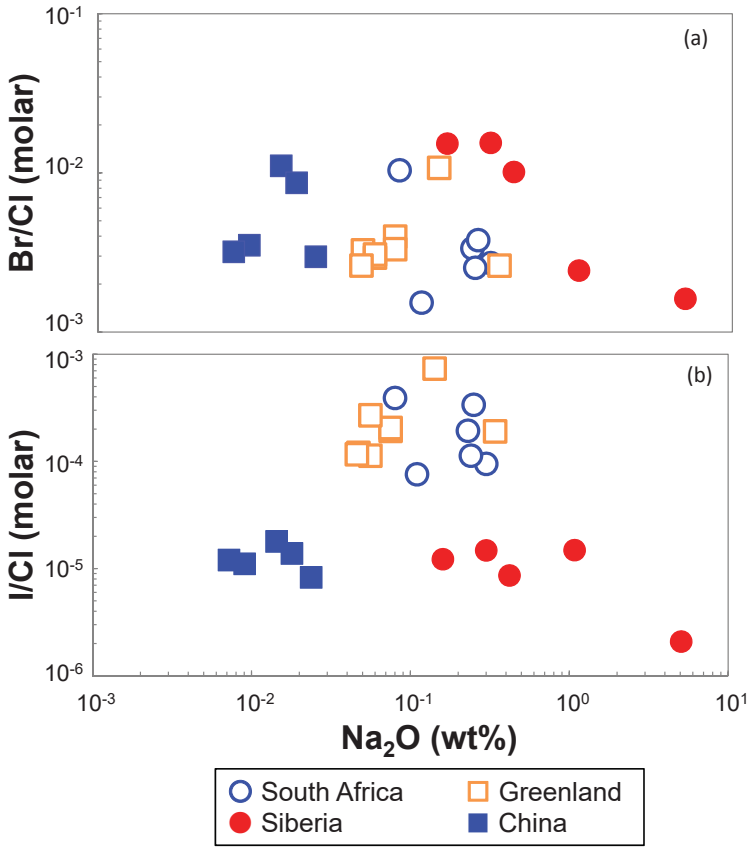

This is the peer-reviewed, final accepted version for American Mineralogist, published by the Mineralogical Society of America.
The published version is subject to change. Cite as Authors (Year) Title. American Mineralogist, in press.
DOI: https://doi.org/10.2138/am-2021-7332. http://www.minsocam.org/

Fig. 5

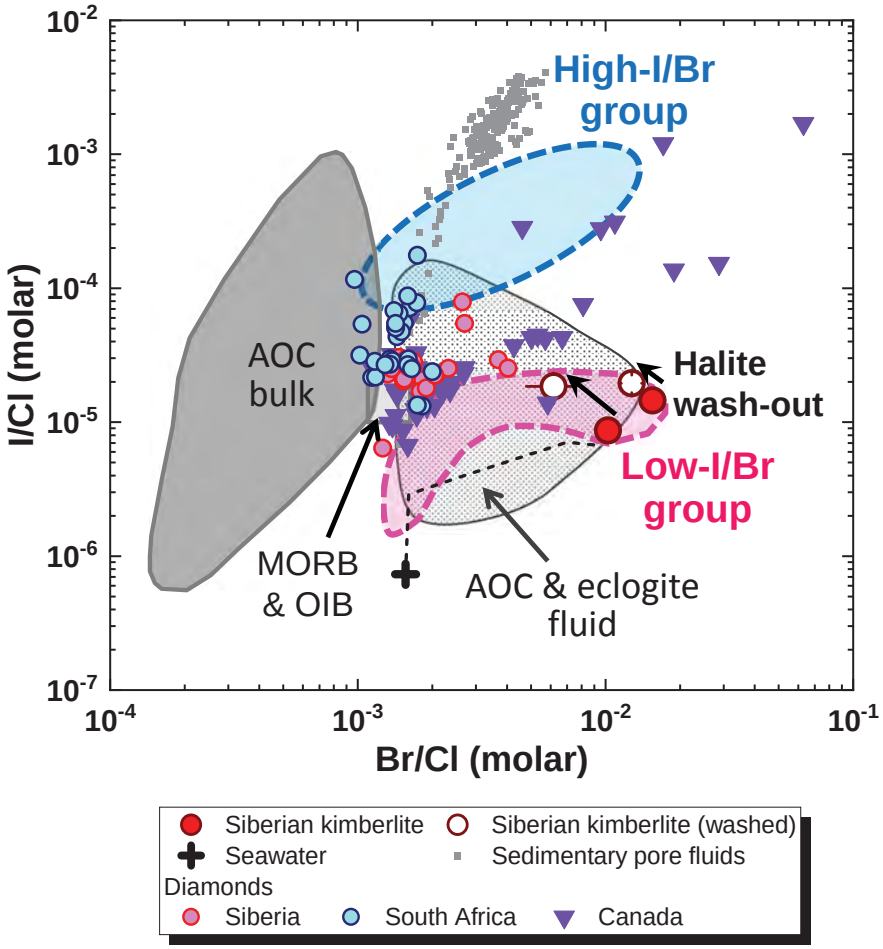

This is the peer-reviewed, final accepted version for American Mineralogist, published by the Mineralogical Society of America.
The published version is subject to change. Cite as Authors (Year) Title. American Mineralogist, in press.
DOI: https://doi.org/10.2138/am-2021-7332. http://www.minsocam.org/

Fig.6